Dicke-Narrowed Line Shapes in CO-Ar: Measurements, Calculations, and a Revised Interpretation

R. Wehr[1], R. Ciuryło[2], A. Vitcu[1], F. Thibault[3], D. A. Shapiro[4], W.-K. Liu[5], F. R. W. McCourt[6], J. R. Drummond[1], and A. D. May[1]

[1]*Dept. of Physics, University of Toronto, Toronto, Canada M5S1A7*
[2]*Institut Fizyki ,Universytet Mikolaja Kopernika, Grudziadzka 5/7 87-100, Torun, Poland*
[3]*UMR 6627 du CNRS, Univ. de Rennes I, Campus de Beaulieu, 35042 Rennes Cedex, France*
[4]*Institute of Automation and Electrometry, Novosibirsk 630090, Russia*
[5]*Dept. of Physics and Astronomy, University of Waterloo, Waterloo, Canada N2L 3G1*
[6]*Dept. of Chemistry, University of Waterloo, Waterloo, Canada N2L 3G1*

Abstract. New line shape calculations for CO buffered by Ar are compared to high-resolution measurements from a difference-frequency laser spectrometer, over a range of thermodynamic conditions relevant to the atmosphere. The calculations are based on solving the quantum kinetic (i.e. transport/relaxation) equation for the molecules within the impact approximation, and rely on the commonly used MOLSCAT [1] and MOLCOL [2] codes to determine the speed-dependent collisional relaxation rate. Velocity-changing effects are treated classically using a rigid sphere potential. The comparison initially reveals that the experimental profiles exhibit only 10% to 30% of the expected Dicke narrowing, which leads us to reevaluate our understanding of the narrowing process. A more subtle aspect of the disagreement between theory and experiment draws our attention to an assumption implicit in the calculation of the collisional relaxation rate: the assumption of a Maxwellian form for the velocity dependence of the off-diagonal elements of the density matrix (i.e. the optical coherences). This assumption allows for an analytical simplification of the problem, but eliminates velocity-changing effects (so that they must be added back in using a supplementary classical calculation, which is based here on a rigid sphere interaction). We find that the removal of the above-mentioned assumption should allow for accurate and fully quantum mechanical (but numerical) line shape calculations for systems like CO-Ar on existing computers.

1. J. M. Hutson and S. Green, *Collaborative Computational Project no. 6 (CCP6)* (UK Science and Engineering Research Council) 1994.
2. D. R. Flower, G. Bourhis, and J.-M. Launay, *Comput. Phys. Commun.*, 131 (2000) 187.

Keywords: Spectral line shape; Quantum calculations; Infrared laser spectroscopy; Dicke narrowing, Collisional narrowing; Collisional broadening; Pressure broadening; Temperature dependence; Carbon monoxide; Inelastic collisions; Statistical correlation.
PACS: 33.70.Jg; 33.20.Ea; 33.20.Vq; 39.30.+w; 42.68.Ca

INTRODUCTION

Infrared absorption line shapes in the atmosphere are typically analyzed using semi-empirical models, the most common example being the Voigt profile. While there are many more complicated examples, accounting for collisional narrowing, speed-

CP874, *Spectral Line Shapes: 18th International Conference,*
edited by E. Oks and M. Pindzola

dependent broadening, and shifting, they are all limited ultimately by their reliance on empirical parameters. Using such models, it is possible to relate the line shape to some previously measured line shape, but it is not possible to predict the line shape from non-spectroscopic information, i.e. directly from the interaction potential, as is the objective of the line shape calculations described here. Owing to the complexity of the problem, there have only ever been a few attempts at a full line shape calculation [1-3], and none has been able to reproduce modern high-resolution spectra within their experimental uncertainties. Note that while there have been many purported calculations of line widths and shifts, these parameters depend on the line shape, and so it is impossible to calculate a width or shift directly in a rigorous way. Rather, the line profile must be calculated first and the width or shift measured from it.

The present study is restricted to isolated rovibrational absorption lines in the fundamental band of carbon monoxide buffered by argon (CO-Ar). We ignore the far wings of the lines and work within the binary impact approximation. CO-Ar was chosen for the present study for several reasons. First, dilutions of CO in Ar simulate the general atmospheric situation, in which infrared-active trace gases are diluted in nitrogen. Second, CO is a diatomic molecule, and thus its rovibrational absorption spectrum is simple, containing well isolated lines that can be measured and analyzed (nearly) independently of one another. Finally, the use of Ar (a structureless atom under atmospheric conditions) as the collision partner simplifies the calculations.

For atmospheric-type systems like CO-Ar, the principal processes contributing to the line shape are collisional broadening and Doppler broadening. However, at the level of accuracy provided by the present spectrometer, it is necessary to consider that the collisional broadening depends on the speed of the active molecule, and that the Doppler broadening is reduced by velocity-changing collisions. The latter effect is known as collisional, or Dicke, narrowing. Collisional line shifting is an order of magnitude weaker than the broadening in CO-Ar [4] and is neglected here (see, however, Ref. [5]). Line mixing is also weak below 1 atm, and the slight asymmetry it introduces into the experimental profiles can be accurately removed using a fitted parameter. Line mixing is thereby omitted from the calculations, in keeping with our focus on isolated lines.

There are a number of other, relatively minor, considerations that are nonetheless significant to the formation of the line shape when it is measured at high resolution. These include, for example: the homogenization of the speed-dependent collisional broadening by speed-changing collisions, the coupling of the collisional broadening and translational motion because they are both speed dependent, the influence of the CO:Ar mass ratio on the velocity memory, and a possible correlation between the velocity-changing and dephasing effects of collisions.[1] In principle, all of these considerations should be included in the present calculations by virtue of our approach, which is first to solve the quantum kinetic equation that describes the interaction of the molecules with each other and with the radiation field, and then to derive the line shape from the solution. However, we shall deliberately remove the correlation between velocity-changing and dephasing collisions from consideration by an approximation that will be discussed below.

[1] The word "dephasing" is used here in a generic sense and includes dephasing, reorienting, and state-changing processes.

In order to test our calculations, we measured the shapes of seven CO-Ar lines in the P branch of the fundamental band using a difference-frequency laser spectrometer. These line spectra were recorded at pressures of 0.025, 0.05, 0.1, 0.2, 0.5, and 1 atm, and at temperatures of 214, 236, 259, 296, and 324 K, thereby covering the thermodynamic conditions found in the Earth's troposphere and lower stratosphere. The particular lines studied were: P(1), P(2), P(5), P(7), P(10), P(13), and P(16). In this paper, we describe first the calculation of the shapes of these lines, and then the experimental apparatus used to measure them. Following that, we present our findings and a discussion of their implications.

CALCULATIONS

To obtain the transport/relaxation equation, we follow Ref. [6] and consider a transition between an initial state *b* and a final state *a* (in the case of photon emission) in the presence of a field represented by $E\exp[-i(\omega t - \mathbf{k}\cdot\mathbf{r})]$, where ω is the frequency and $\mathbf{k}$ is the wavevector. We then write the resonant part ρ_r of the off-diagonal element of the density matrix for the active molecule as $\rho_r = -i\varsigma(\omega,\mathbf{v})n_b\mu_{ba}E\exp[-i(\omega t - \mathbf{k}\cdot\mathbf{r})]$, where n_b is the thermal equilibrium population of state *b*, and μ_{ba} is the matrix element of the electric dipole moment corresponding to a transition between states *b* and *a*. The population of the final state *a* is taken to be zero. Upon making the rotating wave approximation, we arrive at the following transport/relaxation equation [7]:

$$\varsigma_0(\mathbf{v}) = -i(\omega - \omega_0 - \mathbf{k}\cdot\mathbf{v})\varsigma(\omega,\mathbf{v}) - \hat{S}\varsigma(\omega,\mathbf{v}). \qquad (1)$$

Here $\varsigma_0(\mathbf{v})$ is the (typically Maxwellian) velocity distribution of the molecules in state *b* in the absence of the field, ω_0 is the resonant frequency, and $\hat{S}$ is the collision operator. The $\hat{S}$ term contains all the effects of intermolecular collisions, leading to Dicke narrowing and collisional broadening, while the other two terms are "free-streaming" terms. The $\mathbf{k}\cdot\mathbf{v}$ term, in particular, represents the Doppler shift that gives rise to Doppler broadening. The line shape $I(\omega)$ is obtained from $\varsigma(\omega,\mathbf{v})$ as [6]:

$$I(\omega) = \frac{1}{\pi}\mathrm{Re}\int\varsigma(\omega,\mathbf{v})\mathrm{d}^3\mathbf{v}. \qquad (2)$$

In general, the effects of $\hat{S}$ may be difficult to calculate, or even to express in a useful form. One approach (and our approach) is to assume that $\hat{S}$ can be written as $\hat{S} = \hat{S}_{VC} + \hat{S}_D$, where $\hat{S}_{VC}$ is the velocity-changing collision operator, which represents collisions that affect the translational motion, and $\hat{S}_D$ is the dephasing collision operator, which represents collisions that affect the internal relaxation. By writing $\hat{S}$ in this form, one assumes that the effects of collisions on the translational motion and internal relaxation are statistically independent. Eq. (1) then becomes:

$$\varsigma_0(\mathbf{v}) = -i(\omega - \omega_0 - \mathbf{k}\cdot\mathbf{v})\varsigma(\omega,\mathbf{v}) - \hat{S}_{VC}\varsigma(\omega,\mathbf{v}) - \hat{S}_D\varsigma(\omega,\mathbf{v}). \qquad (3)$$

Nearly all line shape models effectively assume that the collision operator can be separated in this way, as they can be derived from Eq. (3) under various simplifying assumptions (see Ref. [8]).

In order to solve Eq. (3), it is converted into a matrix equation using an infinite and complete set of orthonormal basis functions (which is later truncated for numerical calculation). The details of this conversion are provided in Ref. [6]. The result is:

$$\mathbf{L}(\omega) = -\mathrm{i}(\omega - \omega_0)\mathbf{1} + \mathrm{i}\mathbf{K} - \mathbf{S}_{\mathrm{VC}}^{f} - \mathbf{S}_{\mathrm{D}}^{f}, \tag{4}$$

where **1** is the unit matrix, **K** is the Doppler shift matrix, and the $\mathbf{S}^f$ matrices arise from the velocity-changing and dephasing parts of the collision operator. Recipes for **K**, $\mathbf{S}_{\mathrm{VC}}^{f}$, and $\mathbf{S}_{\mathrm{D}}^{f}$ are given in Ref. [7]. For the current study, $\mathbf{S}_{\mathrm{VC}}^{f}$ was calculated classically using a rigid sphere potential for the CO-Ar interaction, while $\mathbf{S}_{\mathrm{D}}^{f}$ was calculated from energy-dependent pressure-broadening cross-sections obtained using the MOLSCAT [9] and MOLCOL [10] quantum mechanical scattering codes, employing the *ab initio* potential energy surface of Toczyłowski and Cybulski [11]. The matrix $\mathbf{L}(\omega)$ was then used to solve the equation $\mathbf{b} = \mathbf{L}(\omega)\mathbf{c}(\omega)$ for the column vector $\mathbf{c}(\omega)$, given that **b** is a column vector whose first element is 1 and whose other elements are 0. Once $\mathbf{c}(\omega)$ is known, the line shape is given by:

$$I(\omega) = \mathrm{Re}\{c_0(\omega)/\pi\}, \tag{5}$$

where $c_0(\omega)$ is the first element of $\mathbf{c}(\omega)$.

More details on the calculations and the computational method can be found in Refs. [1,12] and especially Ref. [13]. Excepting the MOLSCAT and MOLCOL calculations, the calculations described here were performed on a 700 MHz desktop computer, and the calculation of a single line shape took about 10 seconds.

We conclude this section by noting that $\mathbf{S}_{\mathrm{VC}}^{f}$ and $\mathbf{S}_{\mathrm{D}}^{f}$ each contain a physically meaningful parameter that can be factored out of the matrix as a scalar. For $\mathbf{S}_{\mathrm{VC}}^{f}$, this parameter is the effective frequency of velocity-changing collisions, ν, while for $\mathbf{S}_{\mathrm{D}}^{f}$, it is the thermally-averaged collisional relaxation rate, Γ_0. There is no consensus in the literature (see Ref. [12]) as to whether ν should be equal to the dynamic friction coefficient, ν_{diff}, which can be calculated from the mass diffusion constant D via:

$$\nu_{\mathrm{diff}} = \frac{k_{\mathrm{B}}T}{mD}, \tag{6}$$

where k_{B} is the Boltzmann constant, T is the temperature, and m is the mass of the active molecule.[2] For the present calculations, we assumed initially that $\nu = \nu_{\mathrm{diff}}$ and later relaxed that assumption. As for the thermal average, Γ_0, it can be calculated as:

[2] The mass diffusion constant, D, can be related to the diameter, d, of the rigid sphere interaction [7]. However, to maintain contact with the literature, we use D rather than d to characterize the interaction leading to Dicke narrowing.

$$\Gamma_0 = \int_0^\infty f_M(\upsilon)\Gamma(\upsilon)\mathrm{d}\upsilon\,, \tag{7}$$

where υ is the active molecule speed, $f_M(\upsilon)$ is the Maxwellian speed distribution, and $\Gamma(\upsilon)$ is the speed-dependent collisional relaxation rate (obtained from the energy-dependent pressure-broadening cross-section). However, the accuracy with which Γ_0 can be calculated is only ±2% at present, which is the principal limitation on the accuracy of the overall calculation, and is too poor for the analysis of subtle line shape effects such as Dicke narrowing. Therefore, we elected to treat Γ_0 as a fitted parameter. We verify below that our fitted values of Γ_0 agree with our calculated values in their magnitude and their density dependence in all cases – with one important exception that we will discuss in some detail.

MEASUREMENTS

The spectrometer has been described in Refs. [13,14,15], but we repeat some pertinent details here. Two visible laser beams, one of which is tunable, are overlapped in an $LiIO_3$ crystal to generate an infrared (IR) beam at the difference frequency. This beam is split so that one branch passes through a temperature-controlled absorption cell, a second branch passes through a 15 cm long reference cell filled with low pressure CO at room temperature, and a third branch is used to monitor the incident intensity. The reference cell branch is only used to measure line shifts, which are not discussed here. Each branch of the beam is detected by a separate LN_2-cooled InSb detector, and the incident intensity signal is used to normalize the absorption cell signals and thereby remove absorption by laboratory air from the spectra. To detect the relatively weak laser beam against the laboratory's background IR signal, one of the visible laser beams is chopped by an acousto-optic modulator and the detected signals are processed by lock-in amplifiers. The spectrometer is depicted in Fig. 1. It has a frequency uncertainty of less than 1 MHz and a signal-to-noise ratio between 3000:1 and 10,000:1, depending mostly on the effective integration time employed (between 0.5 and 2 seconds).

The temperature-controlled, vacuum-jacketed absorption cell used for the current study was 50 cm long, and used a circulating heat transfer fluid and chiller to regulate the temperature. We were able to set the gas temperature to any value between roughly 210 K and 330 K, with a stability of ±0.1 K. The cell was fitted with CaF_2 windows mounted at Brewster's angle, and with five T-type thermocouples distributed along the length of the cell. Using a combination of the thermocouple measurements and spectroscopic temperature retrievals (following the method of Ref. [16]), we were able to determine the CO-Ar gas temperatures to within ±0.3 K. The gas pressures were recorded with an MKS Baratron capacitance manometer, which was calibrated by the manufacturer immediately before the study and found to be accurate to within 0.05% of the reading. The mixing ratio of CO to Ar was about 0.1%, and thus we can neglect the influence of self-broadening on the speed-dependence of the total broadening.

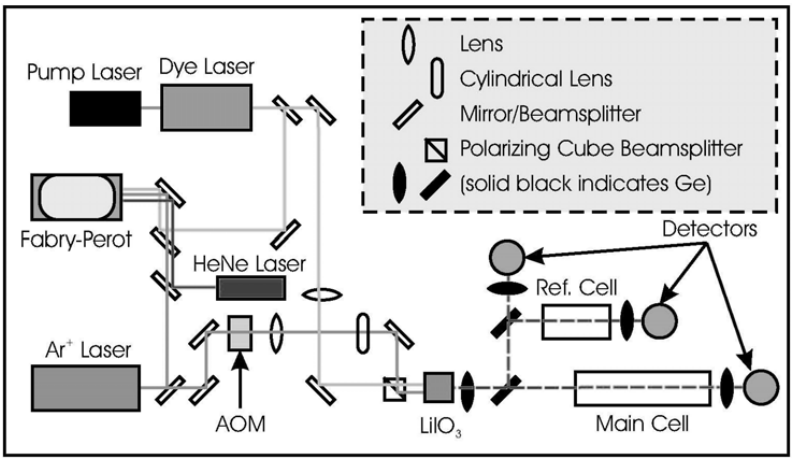

FIGURE 1. Schematic diagram of the difference-frequency laser spectrometer as viewed from above.

FINDINGS

At pressures above 0.2 atm, the line shape is insensitive to Dicke narrowing and is dominated by collisional broadening. For all temperatures and spectral lines in this pressure regime, our calculations (but with Γ_0 fitted) reproduce the measured line shapes within their experimental noise (i.e. within ±0.03% or better). As an example, the residual for the P(13) transition at 1.0 atm and 259 K is shown at the bottom of Fig. 2, underneath the corresponding absorption spectrum. The residual is defined as the difference between the calculated spectrum and the measured spectrum, and agreement between the two is confirmed by the fact that the residual is flat and equal to zero within the experimental noise. (While the spectra are recorded point by point, we have joined the points by straight line segments as a guide to the eye.) Note that there are a number of adjustable parameters used to fit our calculated line shapes to our experimental profiles and produce residuals such as the one shown in Fig. 2. Since our line shape calculation does not include the line strength (i.e. peak height) or the relative frequency of the line centre in a particular experimental scan, it is necessary to fit for those parameters. It is also necessary to fit for a linear baseline slope and intercept. None of these parameters influences the line shape. As mentioned earlier, weak line mixing does introduce a small asymmetry into CO-Ar lines under the conditions studied [1,17], but as we are interested in modelling an isolated line, we exclude line mixing from our calculation and account for the asymmetry with a final fitted parameter. All these fitted parameters are discussed further in Ref. [1]. The broadening and shifting coefficients obtained from our spectra in the > 0.2 atm regime are reported in Ref. [5].

The situation below 0.2 atm, where Dicke narrowing, Doppler broadening, and collisional broadening are all significant, is more problematic. In this pressure regime, when ν is fixed equal to ν_{diff} (as calculated using Eq. (6) and the empirical model of Bzowski et al. [18] for the mass diffusion constant D), we find for all lines and all

temperatures that our line shape calculations fail to reproduce the measured line shapes within their experimental noise. That is true even though Γ_0 is fitted in a least-squares minimization of the residual. As an example, the residual for the P(7) line at 0.05 atm and 296 K is shown in Fig. 3(a), where the 'w' structure near line centre indicates a difference between the measured and calculated shapes. Note that while the maximum value of the residual is only about 1% of the peak absorption, it is well above the noise level as characterized by the fluctuations visible in the line wings.

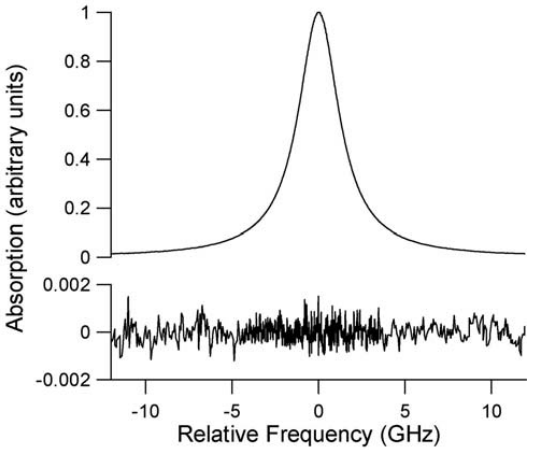

FIGURE 2. Measured spectrum of the P(13) line at 1.0 atm and 259 K (above), and the difference between the calculated spectrum and the measured spectrum (below). Note the expanded vertical scale in the lower plot. The arbitrary absorption units are the same for both plots, and are chosen such that the peak absorption is normalized to 1.

On the other hand, when ν is fitted, the calculations do reproduce the measurements within the experimental noise, as shown in Fig. 3(b). This same agreement is found for all spectral lines at all temperatures and pressures. Note that the increased noise near line centre in Fig. 3(b) should not be confused with structure in the residual. The noise increases because, for this scan, the CO:Ar mixing ratio was slightly higher than desirable, leading to a weak transmission signal at line centre.

The question therefore becomes: what are our fitted values of ν? Before presenting those values, we briefly check whether our fitted values of Γ_0 agree with our calculated values and whether they exhibit the correct physical variation with pressure. Fig. 4 shows a plot of the collisional broadening coefficient, $\gamma_0 = \Gamma_0/P$, versus pressure P for the P(2) line at 296 K. The results when ν is fixed equal to ν_{diff} and when ν is fitted are shown as hollow and solid circles, respectively. On physical grounds, γ_0 should be constant with pressure, as is the case in the $P > 0.2$ atm regime for both the solid and hollow circles. But a non-physical deviation (from a constant high-pressure value) is seen at low pressures in both cases. Fitting ν substantially reduces the deviation in γ_0, but does not eliminate it. The deviation in γ_0 when $\nu = \nu_{diff}$ was discussed in Ref. [1], where it was attributed to an overestimation of the narrowing (the least-squares fitting procedure compensates for an overestimation of the

narrowing by increasing the broadening). That interpretation is supported here by the substantial reduction in the deviation when ν is fitted. However, we also see here that the interpretation of Ref. [1] is only partly correct, as γ_0 is not constant at low pressures even when ν is fitted.

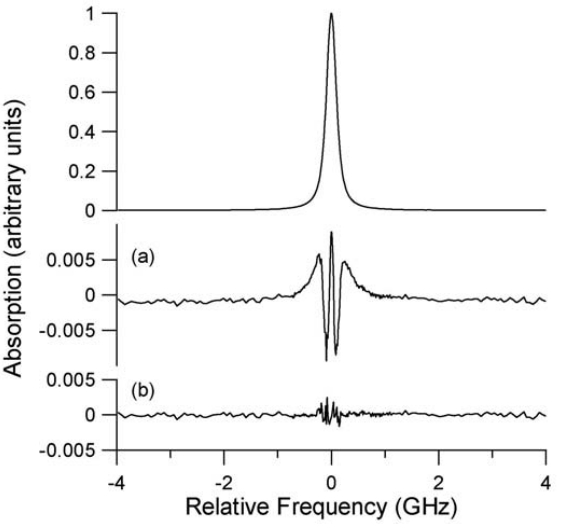

FIGURE 3. Measured spectrum of the P(7) line at 0.05 atm and 296 K, along with residuals (a) when ν is fixed equal to ν_{diff} and (b) when ν is fitted. Note the expanded vertical scale in the residual plots. The arbitrary absorption units are the same for all plots, and are chosen such that the peak absorption is normalized to 1.

The remaining deviation in γ_0 when ν is fitted cannot be attributed to any systematic error in the experiment, because its magnitude varies with temperature such that it is: (1) largest at 259 K, in the middle of the temperature range studied, and (2) negligible at 214 K. The first point makes a systematic error in the temperature or pressure measurement extremely unlikely, while the second point rules out any effect from the instrumental line shape. Thus we conclude that the low-pressure deviation in γ_0 results from some error in our calculation. We return to this point below. In any case, the low-pressure deviation in γ_0 does not affect our fitted values of ν, as will be shown shortly.

We now consider the fitted values of ν. Although there is disagreement in the literature as to the magnitude of ν, there is general agreement that it is proportional to the pressure (e.g. Refs. [19,20]), as expected of a collision rate. Within our experimental uncertainty, we also find ν to be proportional to the pressure, as shown in Fig. 5 for $P \leq 0.1$ atm. At $P \geq 0.2$ atm, the line shape becomes insensitive to ν, and the uncertainty in our retrieved values of ν is too large for those values to be useful. The solid line in Fig. 5 depicts ν_{diff}, which is three to ten times larger than ν, depending on the spectral line. Thus our measured spectra contain less Dicke narrowing than we would predict under the assumption that $\nu = \nu_{diff}$.

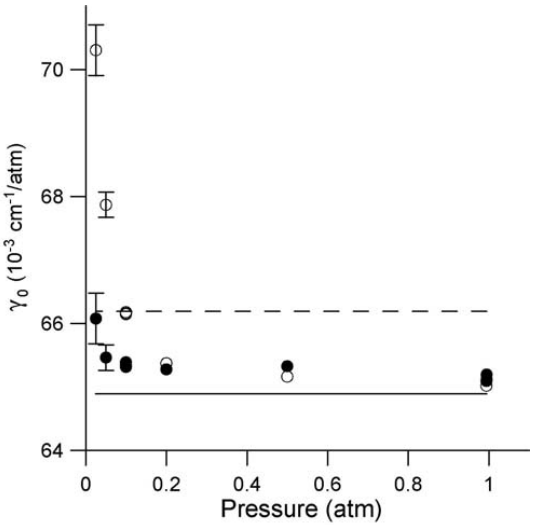

FIGURE 4. Broadening coefficient $\gamma_0 = \Gamma_0/P$ versus pressure P for the P(2) line at 296 K when ν is fixed equal to ν_{diff} (hollow circles) and when ν is fitted (solid circles). The solid horizontal line is the calculated value. The ±2% error in the calculated value is indicated in the positive direction by the dashed horizontal line. The 2σ error bars on the data points are too small to show for pressures above 0.1 atm.

To highlight the reduction of Dicke narrowing in our spectra, we plot in Fig. 6 (lower panel) the ratio ν/ν_{diff} versus rotational quantum number J. The solid triangles in Fig. 6 are our values obtained at 296 K and 0.05 atm. Note that normalizing by ν_{diff} removes the pressure dependence. In units of 10^{-3} cm^{-1}/atm, our calculated values of ν_{diff} are: 31.1 at 214 K, 28.6 at 236 K, 26.5 at 259 K, 23.8 at 296 K, and 22.2 at 324 K. These values should be accurate to within 2.5% [18]. We see from the top panel of Fig. 6 that the variation of Γ_0 with J mirrors that of ν/ν_{diff}, a fact which will be discussed below. As an aside, the hollow circles in Fig. 6 are values obtained when our calculated speed dependence for the collisional broadening is replaced by a fitted, quadratic speed dependence similar to that used in Ref. [14] and other papers. These erroneous values are qualitatively similar to those shown in Fig. 4(a) of Ref. [14], demonstrating the advantage of using a rigorous calculation for the form of the speed-dependent broadening.

In summary, for all spectral lines under all conditions, we find that the Dicke narrowing is reduced relative to what we would predict from the mass diffusion constant. This reduction is not substantially affected by using a soft or hard collision model in place of our rigid sphere calculation (results not shown). Nor is it affected by the low pressure deviation in γ_0 (or equivalently, in Γ_0), as evidenced by the following two facts: (1) unlike Γ_0, ν is proportional to the pressure; and (2) within the precision of the retrieval, the low-pressure values of ν/ν_{diff} at 214 K (where there is no significant deviation in γ_0) agree with the values at 259 K (where the deviation in γ_0 is most pronounced).

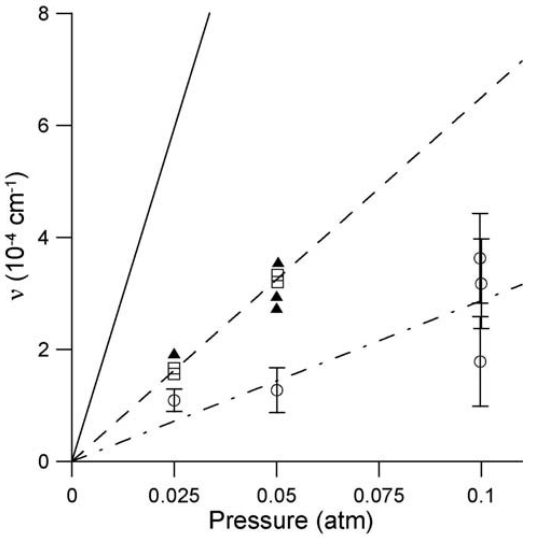

FIGURE 5. Pressure dependence of ν for the P(2) line (circles), the P(7) line (squares), and the P(13) line (triangles), at 296 K. The solid line indicates ν_{diff}, while the dashed line is a linear fit through the origin for P(7) and the dash-dotted line is a linear fit through the origin for P(2). For clarity, 1σ error bars are shown only on the P(2) data points.

DISCUSSION

We are left with two outstanding questions: (1) why do we find less Dicke narrowing in our measured spectra than we calculate from the mass diffusion constant? and (2) why is γ_0 not constant at low pressures even when ν is fitted? We begin with the first question. The model of Rautian and Sobel'man [21] (further developed in Refs. [22,23]), suggests that we overestimate the amount of Dicke narrowing because we separate the collision operator into independent velocity-changing and dephasing parts. By doing so, we neglect the fact that some velocity-changing collisions are really "VCD", or "velocity-changing and dephasing", collisions. Such collisions were also excluded from Dicke's original theory [24], which assumed that "the gas collisions should not influence the internal state of the radiator". It has not been established whether, or to what degree, VCD collisions should contribute to Dicke narrowing in CO-Ar.

To examine this issue, we discard the VC, D, and VCD nomenclature, which is based on intuitive notions of the effects of collisions rather than on a rigorous description of the collision process. Instead, we consider a rigorous decomposition of the collision operator $\hat{S}$, which is provided by Eqs. (2.142-2.148) of Ref. [25]. These equations relate $\hat{S}\rho$ (written there simply as **S**) to quantum mechanical scattering amplitudes by dividing it into a leaving term, $-\mathbf{S}^{(1)}$, and a returning term, $\mathbf{S}^{(2)}$. Adapting the notation of Ref. [25] slightly, $-\mathbf{S}^{(1)}$ is given by:

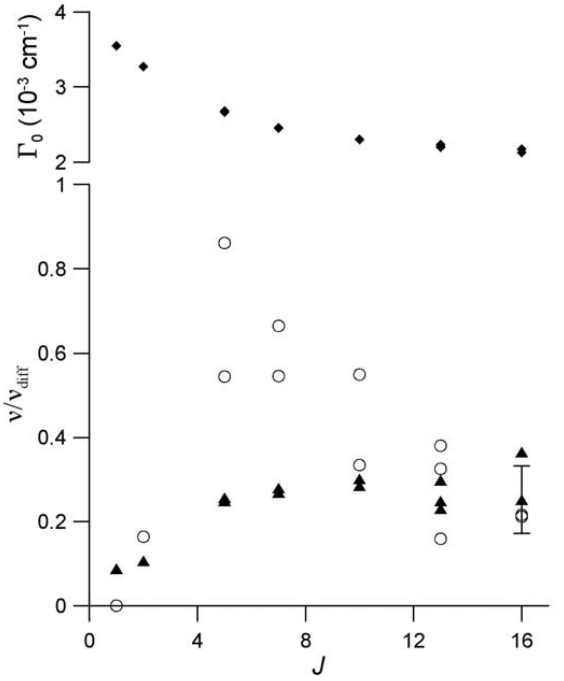

FIGURE 6. ν/ν_{diff} versus J at 0.05 atm and 296 K, as retrieved using our calculated speed dependence for $\Gamma(\upsilon)$ (solid triangles) and using a quadratic, fitted speed dependence instead (hollow circles). 1σ error bars are shown on one of the J = 16 data points. The relaxation rate Γ_0 for the same spectra is shown on the scale above, for comparison. The error bars on Γ_0 are too small to show.

$$-\mathbf{S}^{(1)}(ba,\mathbf{v}) = -\sum_{dc} \nu(ba|dc,\mathbf{v})\rho_{dc}(\mathbf{v}), \tag{8}$$

where *a* and *b* are the lower and upper states, respectively, of the rovibrational transition corresponding to the spectral line of interest; *c* and *d* are those states for some other transition; and ν(ba|dc,**v**) represents the collisional transfer of coherence from the transition *ba* and the velocity **v** to the transition *dc* and all other velocities **v'**. Note that ν(ba|dc,**v**) is more general than the effective frequency of velocity-changing collisions ν in that it includes transfer between components of the optical coherence as well as between velocities. The leaving term $-\mathbf{S}^{(1)}$ therefore involves leaving both to other velocities and to other components of the optical coherence (i.e. to other spectral lines), although only the latter aspect is clear from Eq. (8). The leaving to other velocities can be seen by applying the optical theorem [25, pp. 61 *ff.*] to the forward-scattering amplitudes. The returning term $\mathbf{S}^{(2)}$ is analogous to $-\mathbf{S}^{(1)}$ in that it involves returning both from other velocities and from other components of the optical coherence, but both of these aspects are explicit in the returning term:

$$\mathbf{S}^{(2)}(ba,\mathbf{v}) = \sum_{dc}\int_{\mathbf{v}'} A(ba\mathbf{v}|dc\mathbf{v}')\rho_{dc}(\mathbf{v}')\mathrm{d}\mathbf{v}', \qquad (9)$$

where A(ba**v**|dc**v**') represents the collisional transfer of coherence from the transition *dc* and the velocity **v**' to the transition *ba* and the velocity **v**.

Inspection of Eq. (9) reveals that, in the case of rotationally inelastic collisions (i.e. $dc \neq ba$) [3], the returning from other velocities occurs in the same terms as the returning from other components of the optical coherence. For an isolated line, those terms can be neglected (because, by the definition of an isolated line, ρ_{dc} is negligible at frequencies near the transition *ba* for all $dc \neq ba$), and so the velocity exchange associated with rotationally inelastic collisions cannot homogenize the Doppler broadening. Thus the structure of the collision operator determines that *only rotationally elastic collisions contribute to the Dicke narrowing of an isolated line*. The velocity changes associated with rotationally inelastic collisions still occur, but they do not influence the spectrum. Accordingly, a velocity-changing collision rate based on mass diffusion (i.e. ν_{diff}) will overestimate the effective (elastic) rate ν. Furthermore, since rotationally inelastic collisions are the dominant mechanism for collisional broadening in CO-Ar at atmospheric temperatures [26], we expect large values of Γ_0 to be associated with small values of ν – a "correlation", evident in Fig. 6. The abstention of rotationally inelastic collisions from Dicke narrowing is implied in Ref. [27], in which the returning in velocity is absent in the case of an isolated line, and more recently in Ref. [28], where Dicke narrowing due to rotationally inelastic collisions reappears in the presence of line mixing.

We now turn to our second outstanding question: why is γ_0 not constant at low pressures even when ν is fitted? Since the deviation occurs at low pressure, and increases with decreasing pressure, it is unlikely to result either from an error in the speed-dependent collisional broadening or from an overestimation of speed-class exchange. Errors in either of these two aspects of the calculation ought to become more significant with increasing pressure. The deviation is even less likely to result from an error in the Doppler broadening, which is well understood and trivial to calculate. Our use of a rigid sphere potential to calculate the Dicke narrowing is absolved of responsibility by noting that the deviation is not appreciably affected by replacing our rigid sphere model with a hard or soft collision model (results not shown). So we hypothesize that the deviation occurs because we have oversimplified the collision operator by separating it as in Eq. (3), and because fitting ν is not sufficient to restore the lost information.

In considering this point, it is worth examining the approach by which the dephasing part of the collision operator, $\hat{S}_{\mathrm{D}}$, is calculated. The scattering amplitudes in a binary collision can be calculated using either the MOLSCAT or the MOLCOL software package. In principle, these amplitudes are sufficient to determine all the effects of collisions on the line shape; however, progressing from scattering amplitudes to the line shape is difficult because of the integral nature of the $\mathbf{S}^{(2)}$ term in Eq. (9), with its $\rho(\mathbf{v}')$ dependence (note the prime). That dependence is a feature

[3] By assuming that *a*,*b*,*c* and *d* represent different levels, we are ignoring spatial degeneracy (*m* sublevels). We thus avoid the added complexity of *m*-changing collisions or pure reorientation effects and the problem of complete mixing of lines that are degenerate in the absence of a magnetic field.

common to all Boltzmann-like equations and is the principal reason why analytical solutions have not been found (with the sole exception of Maxwell molecules [29, Ch. 5]). To avoid this problem, the available post-processor codes calculate pressure-broadening cross-sections from the scattering amplitudes based on the Ben-Reuven [30] Shafer-Gordon [31] theory, which gives the line shape only in the high pressure limit (i.e. neglecting Doppler broadening and the effects of velocity-changing collisions on the spectrum). The result of this theory can be obtained from our kinetic theory by employing the ansatz:

$$\rho_{dc}(\omega,\mathbf{v}') = \overline{\rho}_{dc}(\omega) n_{\text{act}} f_{\text{M}}(\mathbf{v}') \tag{10}$$

for some velocity-independent function $\overline{\rho}_{dc}(\omega)$, where n_{act} is the number density of the active molecules and $f_{\text{M}}(\mathbf{v}')$ is the Maxwellian velocity distribution. Substituting Eq. (10) into Eqs. (8) and (9) produces the collisional change

$$\begin{aligned}\int_{\mathbf{v}} \hat{S}\rho_{ba}(\omega,\mathbf{v})\mathrm{d}\mathbf{v} &= \int_{\mathbf{v}} [-\mathbf{S}^{(1)}(ba,\mathbf{v}) + \mathbf{S}^{(2)}(ba,\mathbf{v})]\mathrm{d}\mathbf{v} \\ &= -n_{\text{act}} \sum_{dc} \int_{\mathbf{v}} \left[\nu(ba|dc,\mathbf{v}) - \int_{\mathbf{v}'} A(ba\mathbf{v}'|dc\mathbf{v})\mathrm{d}\mathbf{v}' \right] \overline{\rho}_{dc}(\omega) f_{\text{M}}(\mathbf{v})\mathrm{d}\mathbf{v},\end{aligned} \tag{11}$$

where in the last term, we have interchanged $\mathbf{v}$ with $\mathbf{v}'$ in order to bring out the common factor $f_{\text{M}}(\mathbf{v})$. For an isolated line, we only have $dc = ba$; in that case, by identifying $\rho_{ba}(\omega,\mathbf{v})$ with $\varsigma(\omega,\mathbf{v})$ in Eq. (1), using the ansatz of Eq. (10), and ignoring the $\mathbf{k}\cdot\mathbf{v}$ term (which is negligible compared to the collision term in the high-pressure limit), we obtain a Lorentzian line with a width given by Eq. (7), in which

$$\Gamma(\upsilon) = \nu(ba|ba,\mathbf{v}) - \int_{\mathbf{v}'} A(ba\mathbf{v}'|ba\mathbf{v})\mathrm{d}\mathbf{v}' . \tag{12}$$

More generally, we can define the dephasing contribution as:

$$\mathbf{S}_{\text{D}}(ba,\mathbf{v}) = -\sum_{dc} \left[\nu(ba|dc,\mathbf{v}) - \int_{\mathbf{v}'} A(ba\mathbf{v}'|dc\mathbf{v})\mathrm{d}\mathbf{v}' \right] \rho_{dc}(\mathbf{v}) , \tag{13}$$

which can be computed from an integral over the relative velocity of a binary collision (see Eq. (24) of Ref. [20]) after the appropriate scattering amplitudes have been obtained from MOLSCAT or MOLCOL.[4] To see how this contribution relates to the total collision operator, $\int_{\mathbf{v}'} A(ba\mathbf{v}'|dc\mathbf{v})\rho_{dc}(\mathbf{v})\mathrm{d}\mathbf{v}'$ can now be added to and subtracted from the full colllisional contributions of Eqs. (8) and (9), resulting in:

[4] Here $\mathbf{S}_{\text{D}}$ should not be confused with the corresponding matrix in the section "Calculations".

$$\mathbf{S}(ba,\mathbf{v}) = \mathbf{S}_{\mathrm{D}}(ba,\mathbf{v}) + \sum_{dc}\int_{\mathbf{v}'}\left[A(ba\mathbf{v}|dc\mathbf{v}')\rho_{dc}(\mathbf{v}') - A(ba\mathbf{v}'|dc\mathbf{v})\rho_{dc}(\mathbf{v})\right]d\mathbf{v}'. \quad (14)$$

The term involving the sum and the integral in Eq. (14) is approximated by our $\hat{S}_{\mathrm{VC}}$, which is responsible for Dicke narrowing and whose contribution is calculated here using the classical billiard-ball model. A similar division of $\hat{S}$ has also been carried out in the classical description of Rautian and Sobel'man [21]. Such a separation is not unique, and is useful only if one has reliable models for $\hat{S}_{\mathrm{D}}$ and $\hat{S}_{\mathrm{VC}}$.

The preceding paragraphs are meant not only to explain the low-pressure deviation in our fitted values of γ_0, but also to suggest an approach to performing fully quantum mechanical line shape calculations in the near future. The MOLSCAT and MOLCOL codes already calculate all the quantum mechanical scattering amplitudes required to determine the full collision operator; the limitation has been in obtaining a solution for the off-diagonal density matrix elements responsible for the spectral line shape, i.e. $\rho_{ba}(\omega,\mathbf{v})$. Using today's computers, it should be possible to do so numerically, abandoning Eq. (10). In that case, it would not be necessary to patch Dicke narrowing back into the collision operator with a classical term $\hat{S}_{\mathrm{VC}}$, nor to fit the velocity-changing collision rate ν. The scattering calculations would yield the complete collision operator, including all effects implied by the labels VC, D, and VCD, and the resulting quantum kinetic equation would yield the correct shape for an isolated spectral line. There appears to have been only one attempt along this line [2].

CONCLUSIONS

We have demonstrated that theoretical line shapes obtained by solving the quantum kinetic equation for CO-Ar can reproduce the most accurately measured line shapes available to within their experimental noise, provided that the line shapes are insensitive to the amount of Dicke narrowing present (i.e. for pressures above 0.2 atm). In that case, the line shapes can be calculated *ab initio* except for the thermally averaged relaxation rate Γ_0, which must be fitted to overcome the present limit on the accuracy with which it can be calculated. For pressures at which the line shape is sensitive to the amount of Dicke narrowing (i.e. below 0.2 atm), a comparison between our measured and quantum kinetic line shapes has shown that the magnitude of the Dicke narrowing in CO-Ar is 10% to 30% of that predicted from mass diffusion. Furthermore, an examination of the structure of the collision operator has revealed that the reduced narrowing is probably due to inelastic collisions, which do not cause Dicke narrowing for an isolated line. Finally, we have noted that current quantum mechanical calculations of pressure-broadening cross-sections assume that the velocity dependence of the off-diagonal elements of the density matrix is Maxwellian – an assumption that removes velocity-changing effects from the line shape problem. By abandoning that assumption and solving the problem numerically, it should be possible to calculate the complete line shape quantum mechanically, starting only from the potential energy surface for the CO-Ar interaction.

ACKNOWLEDGMENTS

This work was supported by the Natural Sciences and Engineering Research Council of Canada. The figures and portions of the text herein were originally published by the authors in the Journal of Molecular Spectroscopy [5,12].

REFERENCES

1. R. Wehr, A. Vitcu, R. Ciuryło, F. Thibault, J. R. Drummond, and A. D. May, *Phys. Rev. A* **66,** 062502 (2002).
2. R. Blackmore, S. Green, and L. Monchick, *J. Chem. Phys*. **91** (7), 3846-3853 (1989).
3. L. Demeio, S. Green, and L. Monchick, *J. Chem. Phys.* **102** (23), 9160-9166 (1995).
4. C. Luo, R. Wehr, J. R. Drummond, A. D. May, F. Thibault, J. Boissoles, J.-M. Launay, C. Boulet, J.-P. Bouanich, and J.-M. Hartmann, *J. Chem. Phys*. **115** (5), 2198-2206 (2001).
5. R. Wehr, A. Vitcu, J. R. Drummond, A. D. May, and F. Thibault, *J. Mol. Spectrosc*. **235**, 69-76 (2006).
6. D. A. Shapiro, R. Ciuryło, J. R. Drummond, and A. D. May, *Phys. Rev. A* **65**, 012501 (2001).
7. R. Ciuryło, D. A. Shapiro, J. R. Drummond, and A. D. May, *Phys. Rev. A* **65**, 012502 (2001).
8. A. D. May, *Phys. Rev. A* **59** (5), 3495-3505 (1999).
9. J. M. Hutson and S. Green, *Collaborative Computational Project no. 6 (CCP6)*, UK Science and Engineering Research Council (1994).
10. D. R. Flower, G. Bourhis, and J.-M. Launay, *Comput. Phys. Commun*. **131**, 187-201 (2000).
11. R. R. Toczyłowski and S. M. Cybulski, *J. Chem. Phys*. **112** (10), 4604-4612 (2000).
12. R. Wehr, R. Ciuryło, A. Vitcu, J. R. Drummond, A. D. May, and F. Thibault, *J. Mol. Spectrosc*. **235**, 54-68 (2006).
13. R. Wehr, Dicke-narrowed spectral lines in carbon monoxide buffered by argon, Ph.D. thesis, University of Toronto (2005).
14. P. Duggan, P. M. Sinclair, R. Berman, A. D. May, and J. R. Drummond, *J. Mol. Spectrosc.* **186**, 90-98 (1997).
15. P. Duggan, P. M. Sinclair, M. P. L. Flohic, J. W. Forsman, R. Berman, A. D. May, and J. R. Drummond, *Phys. Rev. A* **48** (3), 2077-2083 (1993).
16. R. Wehr, E. McKernan, A. Vitcu, R. Ciuryło, and J. R. Drummond, *Appl. Opt*. **42** (33), 6595-6604 (2003).
17. R. Berman, P. M. Sinclair, A. D. May, and J. R. Drummond, *J. Mol. Spectrosc.* **198**, 283-290 (1999).
18. J. Bzowski, J. Kestin, E. A. Mason, and F. J. Uribe, *J. Phys. Chem. Ref. Data* **19** (5), 1179-1231 (1990).
19. P. Duggan, P. M. Sinclair, A. D. May, and J. R. Drummond, *Phys. Rev. A* **51** (1), 218-224 (1995).
20. A. S. Pine, *J. Quant. Spectrosc. Radiat. Transfer* **62**, 397-423 (1999).
21. S. G. Rautian and I. I. Sobel'man, *Sov. Phys. Uspekhi* **9** (5), 701-716 (1967).
22. A. S. Pine and R. Ciuryło, *J. Mol. Spectrosc*. **208**, 180-187 (2001).
23. F. Chaussard, X. Michaut, R. Saint-Loup, H. Berger, P. Joubert, B. Lance, J. Bonamy, and D. Robert, *J. Chem. Phys*. **112** (1), 158-166 (2000).
24. R. H. Dicke, *Phys. Rev*. **89** (2), 472-473 (1953).
25. S. G. Rautian and A. M. Shalagin, *Kinetic Problems of Non-Linear Spectroscopy*, New York: Elsevier Science Pub. Co., 1991, p. 43.
26. F. Thibault, R. Z. Martinez, J. L. Domenech, D. Bermejo, and J.-P. Bouanich, *J. Chem. Phys*. **117** (6), 2523-2531 (2002).
27. R. Blackmore, *J. Chem. Phys*. **86** (7), 4188-4197 (1987).
28. V. P. Kochanov, *J. Quant. Spectrosc. Radiat. Transfer* **66**, 313-325 (2000).
29. C. Truesdell, *Indiana Univ. Math. J.* **5** (1), 55-128 (1956).
30. A. Ben-Reuven, *Phys. Rev*. **145**, 7 (1966).
31. R. Shafer and R. G. Gordon, *J. Chem. Phys.* **58**, 5422 (1973).